Fracture Mechanics implications for apparent static friction coefficient in contact problems involving slip-weakening laws

A. Papangelo[1], M. Ciavarella[1], J.R.Barber[2]

[1] Dept. of Mechanics, Mathematics and Management, Politecnico di Bari, Bari - Italy,
  [2] Department of Mechanical Engineering, University of Michigan, Ann Arbor, MI 48109-2125, U.S.A.

Abstract

We consider the effect of differing coefficients of static and dynamic friction coefficients on the behaviour of contacts involving microslip. The classic solutions of Cattaneo and Mindlin are unchanged if the transition in coefficients is abrupt, but if it occurs over some small slip distance, the solution has some mathematical similarities with those governing the normal tractions in adhesive contact problems. In particular, if the transition to dynamic slip occurs over a sufficiently small area, we can identify a 'JKR' approximation, where the transition region is condensed to a line. A local singularity in shear traction is then predicted, with a stress-intensity factor that is proportional to the the square root of the local contact pressure and to a certain integral of the friction coefficient-slip distance relation. We can also define an equivalent of the 'small-scale yielding' criterion, which enables us to assess when the singular solution provides a good approximation. One consequence of the results is that the static coefficient of friction determined from force measurements in experiments is significantly smaller than the value that holds at the microscale.

1 Introduction

If a deformable structure with frictional interfaces is subjected to loads that are insufficient to cause gross slip (sliding), the deformation of the components generally permits some local regions of 'microslip' at the nominally stuck contact interfaces. When the loading is periodic, these regions contribute to the energy dissipation in the structure and hence influence the dynamic behaviour [1, 2]. Also, cyclic microslip can eventually lead to the initiation and propagation of fretting fatigue cracks [3].

Most of the extensive literature on problems involving microslip assumes that Coulomb's friction law applies — i.e.

$$\boldsymbol{q} = -fp\frac{\dot{\boldsymbol{u}}}{|\dot{\boldsymbol{u}}|} \; ; \quad \dot{\boldsymbol{u}} \neq 0 \tag{1}$$

$$|\boldsymbol{q}| \leq fp \; ; \qquad \dot{\boldsymbol{u}} = 0 \; , \tag{2}$$

where $\boldsymbol{q}$ is the frictional (tangential) traction, p is the contact pressure, $\dot{\boldsymbol{u}}$ is the local microslip velocity, and f is the coefficient of friction. In particular, it

is usually assumed that the same coefficient f governs both the slip and stick regions.

By contrast, dynamicists and tribologists often make a distinction between static and dynamic friction [4], so that equations (1,2) are replaced by

$$\boldsymbol{q} = -f_d\, p\, \frac{\dot{\boldsymbol{u}}}{|\dot{\boldsymbol{u}}|}\;;\quad \dot{\boldsymbol{u}} \neq 0 \tag{3}$$

$$|\boldsymbol{q}| \leq f_s\, p\;;\qquad \dot{\boldsymbol{u}} = 0\;, \tag{4}$$

where f_s, f_d are the static and dynamic friction coefficients respectively. In particular, if $f_s > f_d$, this friction law provides a mechanism for 'stick-slip' frictional vibrations [5]. Numerous experimental investigations have shown differences between static and sliding friction (e.g. [6]). These differences are generally small for dry metals [7], but can be substantial for earthquake fault mechanics, where ratios as high as ten between the coefficients have been reported [8]. Rice [9] characterizes such interfaces as 'strong but brittle'.

A higher coefficient of static friction can to some extent be explained by noting that the formation of adhesive bonds, which forms the basis of Bowden and Tabor's friction theory [10], will be enhanced by diffusion if asperities remain in contact for some period of time. Similar arguments can be used to justify the 'rate-state' friction model [11, 12]

In this paper, we shall examine the effect of introducing a higher coefficient of static friction on problems involving microslip. In the interests of simplicity, we shall restrict attention to cases where Dundurs' parameter $\beta = 0$ ([13] p. 110), so there is no coupling between normal and tangential loading, and the contact pressure can be determined without reference to the friction law. Also, we shall illustrate our ideas in the context of the two-dimensional Hertz problem, since this is susceptible to simple analytical solutions, but extension to other two-dimensional cases, and to the axisymmetric Hertz problem is routine.

2 Evolution of frictional traction distributions

Cattaneo [14] and later Mindlin [15] considered the case where two elastic bodies are first pressed together by a normal force P, which is then held constant whilst a monotonically increasing unidirectional force Q_x is applied. The profile of the bodies was characterized by a quadratic initial gap function $g_0(x,y) = Ax^2 + By^2$, so that the normal loading phase is defined by the classical Hertz theory. Cattaneo and Mindlin then showed that, subject to a small approximation associated with the local slip direction [16], the shear traction distribution has the form

$$q_x(x,y) = f\left[p(x,y) - p^*(x,y)\right]\;, \tag{5}$$

where $p(x,y)$ is the contact pressure and $p^*(x,y)$ is the contact pressure that would be developed at some smaller normal force P^* given by

$$P^* = P - \frac{Q_x}{f}\;. \tag{6}$$

Ciavarella [17] and Jäger [18] have since shown that this form of superposition is exact for any initial gap function $g_0(x)$ in the two dimensional case, and that it is a good approximation in the general three-dimensional case [19].

3 Static and dynamic friction

Now consider the case where $f_s > f_d$ and the loading scenario is the same as in the Cattaneo-Mindlin problem. We assume the existence of a slip zone in which $q_x(x,y) = f_d\, p(x,y)$, so we write the complete shear traction distribution as

$$q_x(x,y) = f_d\, p(x,y) - q_x^*(x,y)\;, \tag{7}$$

where $q_x^*(x,y)$ is a corrective distribution to be determined from the condition that the slip displacement (i.e. the relative tangential displacement) is zero in the stick area $\mathcal{A}_{\text{stick}}$. Conditions (3,7) require that $q_x^*(x,y)$ be non-zero only in $\mathcal{A}_{\text{stick}}$, and hence the stick condition defines a well-posed boundary-value problem for $q_x^*(x,y)$. The inequality condition (4) precludes singularities in the shear tractions, and this imposes uniqueness on the solution for any given $Q_x < f_d\, P$. It is clear that the original Cattaneo-Mindlin solution (5) with $f = f_d$ satisfies these conditions, including the inequality, since in $\mathcal{A}_{\text{stick}}$, this would give $q_x(x,y) < f_d\, p(x,y) < f_s\, p(x,y)$.

4 Dependence on slip distance

The discussion so far is predicated on the assumption that as soon as stick is 'broken' there is an immediate transition to the dynamic coefficient f_d, but in practice we might expect a more continuous transition as slip occurs. We shall therefore examine the consequences of a friction law in which the coefficient of friction is a continuous and monotonic function $f(u)$ of the slip displacement u, such that

$$f(0) = f_s \quad \text{and } f(u) \to f_d\;;\quad u \to \infty\;. \tag{8}$$

Such a law can be regarded as a special case of the rate-state law [11, 12] and is also related to the the shear failure law proposed by Abercrombie and Rice [20]. Applications of similar laws to fault mechanics are discussed by Ben Zion [21].

   In general, solutions of the corresponding contact problem will then require numerical solution, but it is instructive to consider some simple cases analytically. In particular, we shall consider the two-dimensional case where the bodies comprise a cylinder of radius R and a half space, so the contact pressure is given by

$$p(x) = \frac{E^*\sqrt{a^2 - x^2}}{2R}\;;\quad P = \frac{\pi E^* a^2}{4R}\;, \tag{9}$$

where a is the semi-width of the contact area $-a < x < a$, and E^* is the composite elastic modulus [13].

3

We anticipate the existence of two symmetric slip regions $-a < x < -c$ and $c < x < a$ in which the slip displacement increases monotonically away from the stick-slip boundaries $x = \pm c$. Two limiting cases can also be identified. If $f(u)$ is a rather slowly decaying function of u, the friction coefficient will be close to f_s throughout the slip regions and the solution will approximate the constant coefficient case with $f = f_s$. At the other limit, if a very small amount of slip displacement is required to precipitate the change in coefficient, most of the slip area will be at or near f_d, but we must still allow for the existence of 'transition' regions $c < |x| < b$ in which $f > f_d$.

The exact form of the function $f(u)$ is not critical, but it is convenient to define a quantity W with the dimensions of surface energy through the relation

$$W = \int_0^\infty (f(u) - f_d)p\,du \,, \tag{10}$$

which is equivalent to the shear fracture energy defined by Abercrombie and Rice [20]. The contact pressure p will generally vary in the transition region, but if this is sufficiently short for p to be regarded as uniform, we can also define a length scale Δ characterizing the amount of slip needed to transition to dynamic friction, such that

$$\Delta = \frac{W}{(f_s - f_d)p} = \frac{1}{(f_s - f_d)} \int_0^\infty (f(u) - f_d)\,du \,. \tag{11}$$

Rabinowicz [6] conducted some simple but elegant experiments to determine f_s, f_d and Δ for metals, his results[1] being presented in Table 1.

Materials	f_s	f_d	Δ (μm)
copper/mild steel	0.46	0.31	1
lead/mild steel	0.72	0.47	3
mild steel/copper	0.54	0.39	0.9
mild steel/titanium	0.63	0.45	6
mild steel/zinc	0.65	0.47	2

Table 1: Friction coefficients and slip length Δ for some metal combinations, from [6]

A special case satisfying equations (10, 11) is the step function $f = f_s - (f_s - f_d)H(u - \Delta)$, where $H(\cdot)$ is the Heaviside step function. The perceptive reader will notice a similarity here to Maugis' approximate formulation of the normal adhesive contact problem [22], where the adhesion law is also represented by a step function and the outer boundary of the adhered region is determined from the condition that the separation there is equal to a critical value. Indeed we shall see that there are significant mathematical analogies between the present problem and adhesive problems.

---

[1]It is difficult to explain why different results might be obtained by simply interchanging the materials in the mild steel/copper case, but the difference is arguable within the range of likely experimental variance.

4.1 A double-Cattaneo-Mindlin solution

The present problem could be formulated using a step function for $f(u)$, but a simpler mathematical approximation can be obtained by adapting the 'double-Hertz' concept of Greenwood and Johnson [23]. We first note that the Cattaneo-Mindlin traction distribution $q_x(x) = q(x, a, c), Q_x = Q(a, c)$, where

$$q(x, a, c) = \sqrt{a^2 - x^2} - \sqrt{c^2 - x^2} \; ; \quad Q(a, c) = \frac{\pi(a^2 - c^2)}{2} \tag{12}$$

produces slip displacements $u_x(x)$, such that

$$\frac{\partial u_x}{\partial x} \equiv v(x, a, c) \quad = \quad 0 \; ; \qquad\qquad -c < x < c \tag{13}$$

$$= \quad -\frac{2\sqrt{x^2 - c^2}}{E^*} \quad ; \; c < |x| < a \tag{14}$$

([13] p. 214), where the square roots in (12) are to be interpreted as zero in any region where their respective arguments are negative.

We next approximate the solution to the frictional problem as

$$q_x(x) = \frac{E^* f_d \, q(x, a, c)}{2R} + Cq(x, b, c) \; ; \quad Q_x = \frac{E^* f_d \, Q(a, c)}{2R} + CQ(b, c) \; , \tag{15}$$

where $c < b < a$. The corresponding slip displacements will then satisfy

$$\frac{\partial u_x}{\partial x}(x) = \frac{E^* f_d \, v(x, a, c)}{2R} + Cv(x, b, c) \; , \tag{16}$$

and this is zero in $-c < x < c$ from (13), showing that the stick condition can be satisfied by an appropriate rigid-body translation.

The shear tractions in $b < |x| < a$ are

$$q_x(x) = \frac{E^* f_d \, \sqrt{a^2 - x^2}}{2R} = f_d \, p(x) \; , \tag{17}$$

and hence satisfy the slip condition at $f = f_d$, since the other square-root terms make no contribution in this range. In $c < |x| < b$, the shear tractions are

$$q_x(x) = f_d \, p(x) + C\sqrt{b^2 - x^2} \; , \tag{18}$$

and we can choose the constant C so as to ensure that $q_x(c) = f_s \, p(c)$, giving

$$C = \frac{E^*(f_s - f_d)}{2R} \sqrt{\frac{a^2 - c^2}{b^2 - c^2}} \tag{19}$$

and

$$q_x(x) = \frac{E^* f_d \, q(x, a, c)}{2R} + \frac{E^*(f_s - f_d)}{2R} \sqrt{\frac{a^2 - c^2}{b^2 - c^2}} \, q(x, b, c) \; . \tag{20}$$

5

With this choice, the effective local coefficient of friction $f = q_x/p$ will decrease monotonically from f_s to f_d in $c < |x| < b$.

The final step is to determine the unknown radii c, b from the equilibrium condition $(15)_2$, and from (10) which we can write as

$$W = \int_c^b [q_x(x) - f_d\, p(x)]\, \frac{du_x}{dx} dx \;. \tag{21}$$

In $c < |x| < b$, we have

$$\frac{du_x}{dx} = -\frac{1}{R}\left(f_d + (f_s - f_d)\sqrt{\frac{a^2 - c^2}{b^2 - c^2}}\right)\sqrt{x^2 - c^2}\;, \tag{22}$$

from (14,19). Using this expression and (18) in (21) and evaluating the integral, we obtain

$$
\begin{aligned}
W &= -\frac{E^* b(f_s - f_d)}{6R^2}\sqrt{\frac{a^2 - c^2}{b^2 - c^2}}\left(f_d + (f_s - f_d)\sqrt{\frac{a^2 - c^2}{b^2 - c^2}}\right) \\
&\quad \times \left[(b^2 + c^2)E(k) - 2c^2 K(k)\right]\;,
\end{aligned}
\tag{23}
$$

where

$$k^2 = 1 - \frac{c^2}{b^2} \tag{24}$$

and

$$K(k) = \int_0^{\pi/2} \frac{d\theta}{\sqrt{1 - k^2 \sin^2\theta}}\;; \quad E(k) = \int_0^{\pi/2} \sqrt{1 - k^2 \sin^2\theta}\, d\theta \tag{25}$$

are the complete elliptic integrals of the first and second kind respectively. The equilibrium condition is obtained from (12,15,19) as

$$Q_x = \frac{\pi E^*}{4R}\left[f_d(a^2 - c^2) + (f_s - f_d)\sqrt{(b^2 - c^2)(a^2 - c^2)}\right]\;. \tag{26}$$

If Q_x, W are given, (23, 26) provide two equations for the two unknown radii c, b.

4.2 The 'JKR' limit

If the transition from f_s to f_d occurs over a sufficiently small region, we can obtain a limiting solution analogous to the JKR solution of normal adhesion problems. We write $b = c + \delta$, where $\delta \ll c$, in which case (23) can be approximated as

$$W \approx \frac{\pi E^*(f_s - f_d)^2(a^2 - c^2)\delta}{16R^2} \quad \text{implying} \quad \delta \approx \frac{16R^2 W}{\pi E^*(f_s - f_d)^2(a^2 - c^2)}\;. \tag{27}$$

Also, the second term in $q_x(x)$ in equation (15) can be approximated as

$$Cq(x, b, c) \approx Cq(x, c, c) + C\delta\frac{\partial q}{\partial a}(x, c, c) = \frac{Cc\delta}{\sqrt{c^2 - x^2}} . \qquad (28)$$

Applying the same approximation to equations (19, 26) and substituting for δ from (27), we obtain

$$q_x(x) \approx \frac{E^* f_d\, q(x, a, c)}{2R} + \sqrt{\frac{2WE^* c}{\pi(c^2 - x^2)}} , \qquad (29)$$

and

$$\frac{Q_x}{f_d P} = \frac{4RQ_x}{\pi E^* f_d a^2} \approx 1 - \frac{c^2}{a^2} + \frac{4R}{f_d\, a^2}\sqrt{\frac{2Wc}{\pi E^*}} . \qquad (30)$$

Equation (29) defines a locally singular field, implying the existence of a mode II stress-intensity factor

$$K_{\mathrm{II}} \equiv \lim_{x \to c^-} q_x(x)\sqrt{2\pi(c - x)} = \sqrt{2WE^*} , \qquad (31)$$

which is exactly analogous with the mode I stress intensity factor $K_{\mathrm{I}} = \sqrt{2\Delta\gamma E^*}$ in normal adhesion problems in the JKR limit, where $\Delta\gamma$ is the interface energy.

In an impressive series of experiments, Svetlizky and Fineberg [24] have observed frictional slip progressing by the relatively slow propagation of slip zones behind which the shear tractions approximate a square-root singularity. The strength of this singularity is approximately constant, indicating a well-defined value of fracture energy W, but they suggest it may depend on the local pressure, as a result of the area of actual contact being approximately proportional to pressure.

Ciavarella [25] presented solutions of contact problems with a mode II stress-intensity factor around the stick-slip boundary, motivated by Fineberg's observations. The present analysis shows that such an effect can be generated by a slip-dependent friction law of the form (8) and provides a rationale for determining an appropriate value of K_{II}. In particular, we notice from (31) that the stress-intensity factor depends only on the composite modulus and W, and is otherwise independent of the details of the contact problem. Since *ex hypothesi*, the transition is assumed to occur over a small region (of width δ) in the contact area, we can assume that the contact pressure p is uniform in this region, and hence use the form (11) for W. This leads to a stress-intensity factor

$$K_{\mathrm{II}} = \sqrt{2E^*(f_s - f_d)p\Delta} , \qquad (32)$$

which varies with $\sqrt{p}$ and is equivalent to the 'pressure-dependent toughness' criterion of [25].

Using (11) to recast equations (29, 30) in terms of Δ, we have

$$q_x(x) \quad \approx \quad \frac{E^* f_d \, q(x, a, c)}{2R} + E^* \sqrt{\frac{(f_s - f_d)\Delta c \sqrt{a^2 - c^2}}{\pi R(c^2 - x^2)}} \tag{33}$$

$$\frac{Q_x}{f_d P} \quad \approx \quad 1 - \frac{c^2}{a^2} + \frac{4}{f_d \, a^2}\sqrt{\frac{(f_s - f_d)R\Delta c \sqrt{a^2 - c^2}}{\pi}} \; . \tag{34}$$

4.3 Small-scale transition zone

Equation (32) implies that at a sufficiently small distance s from the stick boundary, the frictional tractions have the singular form

$$q_x(s) \approx f_d p + \sqrt{\frac{E^*(f_s - f_d)p\Delta}{\pi s}} \; . \tag{35}$$

However, this expression violates the stick condition (4) in the region $0 < s < s_0$, where

$$\sqrt{\frac{E^*(f_s - f_d)p\Delta}{\pi s_0}} = (f_s - f_d)p \quad \text{or} \quad s_0 = \frac{E^*\Delta}{\pi(f_s - f_d)p} \; . \tag{36}$$

An analogous situation is encountered in elastic-plastic fracture mechanics, where the 'small-scale yielding' criterion is used to determine whether the fields far outside the yield zone can reasonably be described by the elastic solution [26]. In the present case, the singular solution can be expected to give good results everywhere except very close to $x = c$, provided $s_0 \ll c$.

This criterion depends on c and hence on Q_x, but a rough estimate of the applicability of the JKR solution in the present problem can be obtained by using $p(0), a$ for p, c respectively, defining the modified criterion

$$\Lambda \equiv \frac{R\Delta}{(f_s - f_d)a^2} \ll 1 \; . \tag{37}$$

4.4 More general two-dimensional problems

We have analyzed the two-dimensional Hertzian problem in detail because the resulting expressions are algebraically straightforward, enabling the fundamental structure of the solution to be exposed. However, the same method can be applied to any two-dimensional problem involving a single symmetric contact area. We simply replace equation (12) by

$$q(x, a, c) = p(x, a) - p(x, c) \; ; \quad Q(a, c) = P(a) - P(c) \; , \tag{38}$$

where $p(x, a)$ is the normal contact pressure when the contact area is defined by $-a < x < a$, and $P(a)$ is the corresponding normal force. We know from Ciavarella [17] and Jäger [18] that this will satisfy equation (13), so the traction distribution

$$q_x(x) = f_d q(x, a, c) - C q(x, b, c) \tag{39}$$

8

will satisfy the stick conditions in $-c < x < c$ and the dynamic slip conditions in $b < |x| < a$. The rest of the solution can then be completed as in §4.1.

If the length scale s_0 in (36) is sufficiently small to justify the JKR approximation, the second term will take the universal form (28), so the solution can be written down as the superposition of a conventional Cattaneo-Mindlin solution with coefficient of friction f_d and equation (28). In this context, it may be helpful to note that the limiting expression for $Q(b, c)$ is

$$Q(b, c) = \int_{-c}^{c} Cq(x, b, c)dx \to \sqrt{2\pi W E^* c} \,, \tag{40}$$

so the total tangential force is

$$Q_x = f_d \left[P(a) - P(c) \right] + \sqrt{2\pi W E^* c} \,. \tag{41}$$

Since Q_x will usually be prescribed, this provides an equation from which c can be determined as a function of Q_x.

5   Finite element results

The double Cattaneo-Mindlin solution is approximate in the sense that we are able to match a specific value of the fracture energy W or (equivalently) the length scale Δ, but the exact form of the function $f(u)$ cannot be prescribed. The implied form of this function depends on the dimensionless ratios $b/c, a/c$, some representative curves being shown as dashed and dotted lines in Fig. 1.
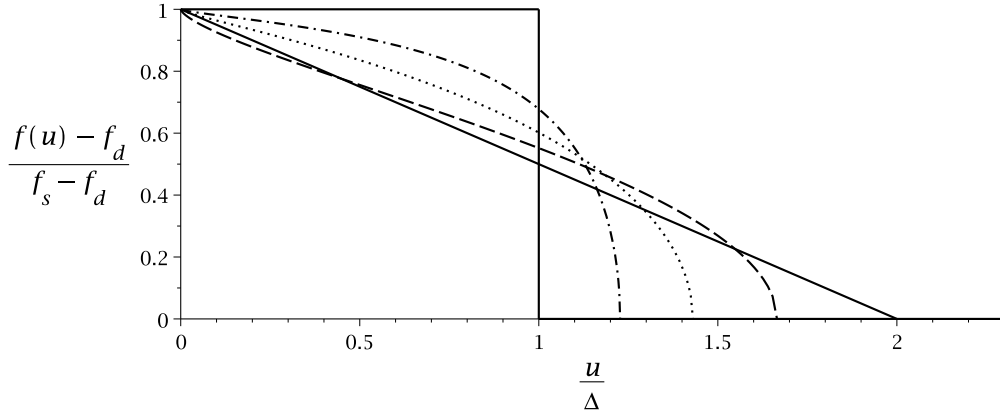

Fig. 1: The friction coefficient function $f(u)$ implied by the double Cattaneo-Mindlin solution for $a/c = 1.6, b/c = 1.5$ (— · — · —), $a/c = 8.0, b/c = 4.5$ (· · · ·), $a/c = 8.0, b/c = 1.2$ (— — —).

To assess the effect of this approximation, we constructed a finite element solution of the problem, as an extension of the "verification manual" VM272

example in Ansys 15 [27], which in turn is based on the method of Yang *et al.* [28] and an example given therein which compares satisfactorily with the analytical Cattaneo-Mindlin solution. It is based on a mortar formulation of the contact which is able to deal with nonconforming discretizations across boundaries and large sliding which is more than adequate for our problem. In [28], several examples and comparisons are made to show that this method has an optimal convergence rate and robustness with respect to other approaches. The example considers two parallel linear elastic half cylinders of radius R and pressed by a small distributed pressure on the diameter. A tangential pressure is then applied to cause friction at the contact interface, while the top of the upper cylinder is constrained from rotating. The bottom of the lower cylinder is fixed in all directions. The standard input listing available in ANSYS is adequate for many problems, but two minor changes made in the present case were:-

1. We used quadratic PLANE183-CONTA172 instead of linear elements PLANE182-CONTA171, and we modified the mesh parametrically keeping the same ratio of elements, in order to improve marginally the accuracy of the results. For the figures reported in the paper we divided every element edge by 3 which brings the total number of elements to about 45000, but still permits a solution of an entire curve of loading in less than a minute.

2. We did not use the ANSYS variant of the friction law with just static and dynamic coefficients, since this does not permit a dependence on slip displacement. Instead., we defined a table of friction coefficients in terms of slip displacement.

Fig. 2 compares the shear traction $q_x(x)$ from equation (20) for $Q_x = 0.8 f_d P$, $f_s = 0.15, f_d = 0.1, \Lambda = 0.05$, with finite element results using the ramp (linear) function for $f(u)$ from Fig. 1. The agreement is clearly extremely good. Also shown on this figure are the conventional Cattaneo-Mindlin prediction (equivalent to taking $\Delta = 0$) and the JKR approximation (33). The latter gives good predictions everywhere except in the transition region, where of course the predicted singular stress is unphysical.
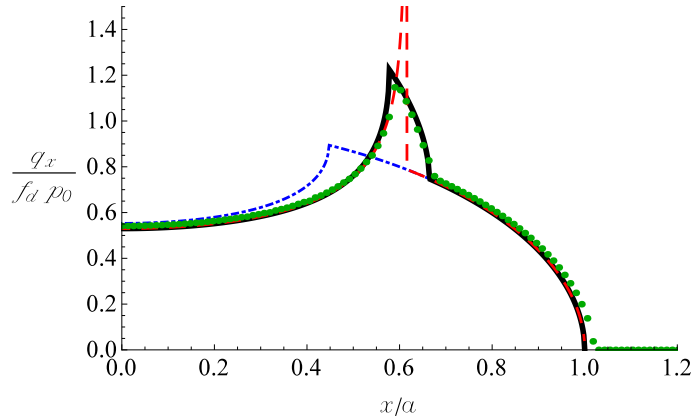
Fig. 2: Finite element results ($\bullet\bullet\bullet$) for the shear traction distribution $q_x(x)$ for $Q_x = 0.8 f_d P, f_s = 0.15, f_d = 0.1$ and $\Lambda = 0.05$: ▬▬ Double Cattaneo-Mindlin solution (20), ▬·▬·▬ Conventional Cattaneo-Mindlin solution (5) with $f = f_d$, ▬ ▬ ▬ 'JKR' approximation of equation (33).

Fig. 3 shows a similar comparison for a larger value of Δ, so that the transition extends over a larger radius. In this figure, we compare equation (20) with finite element solutions using the ramp function and the step function respectively from Fig. 1. This figure shows that the traction distribution is relatively insensitive the the form of the function $f(u)$ for given values of $(f_s - f_d)$ and Δ, and hence that equation (20) can be expected to give good results for most practical slip-weakening laws.
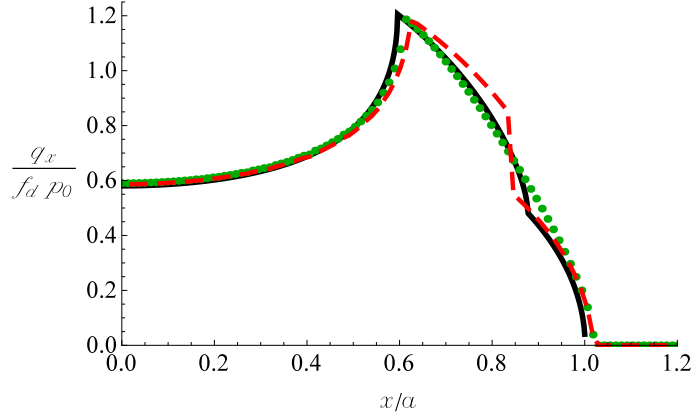

Fig. 3: Effect of the function $f(u)$ on the traction distribution $q_x(x)$: $\bullet\bullet\bullet$ ramp (finite element), ▬ ▬ ▬ step (finite element), ▬▬ equation (20). $Q_x = 0.9 f_d P$, $f_s = 0.15, f_d = 0.1, \Lambda = 0.277$.

6 Discussion

The principal new result from this analysis is that fracture mechanics concepts are introduced into the microslip problem, even when the friction law is merely an extension of the Coulomb law allowing differing static and dynamic coefficients. In particular, if the coefficient of friction varies with slip dispacement over a relatively short slip distance Δ, we can determine a critical stress intensity factor or fracture toughness (32) that depends only on the static and dynamic coefficients, the form of the slip-weakening law, the composite modulus and the local contact pressure.

Equation (34) defines the relation between tangential force Q_x and the semi-length c of the stick area in the JKR limit, which is appropriate if the small-scale transition criterion $s_0 \ll c$ is satisfied. It is plotted in Fig. 4 for several values

of the dimensionless parameter

$$\Psi = \left(\frac{f_s}{f_d} - 1\right)\frac{R\Delta}{f_d a^2} = \left(\frac{f_s}{f_d} - 1\right)^2 \Lambda \ . \tag{42}$$
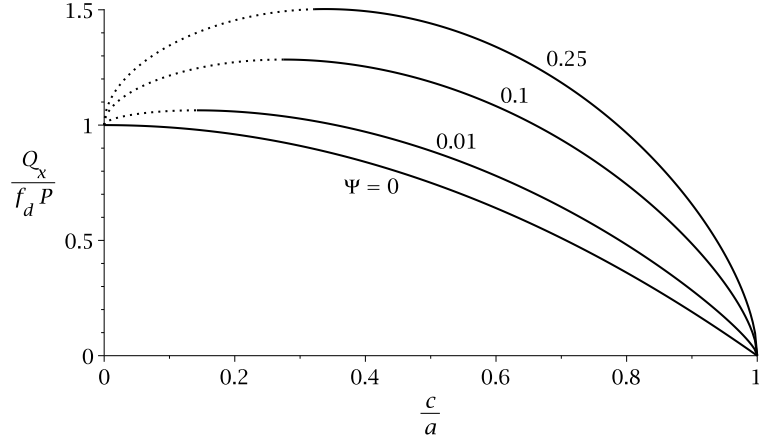

Fig. 4: The tangential force Q_x as a function of the radius c of the stick zone (JKR limit).

All the curves except the limiting case $\Psi = 0$ exhibit a maximum $Q_x = Q_{\max}$ at a non-zero value of c, implying that under tangential force control, the system would jump unstably to full sliding once this maximum is reached. The unstable range is shown dotted in Fig. 4.

Similar plots were made for the double Cattaneo-Mindlin solution, using equations (26, 23) with $W = (f_s - f_p)\Delta$. Fig. 5 compares the resulting curves for $\psi = 0.1$ and $\Lambda = 0.025, 0.4$ with the JKR solution. Notice that changing Λ at constant ψ implies a change in the friction coefficient ratio f_s/f_d. The truncation in these curves near $c = a$ occurs because the outer boundary b of the transition region cannot exceed the boundary a of the contact area. When $b = a$, the double Cattaneo-Mindlin solution reduces to a conventional Cattaneo-Mindlin solution with $f = f_s$, so we have arbitrarily used this result to continue the curves to $c = a$ [shown dotted].
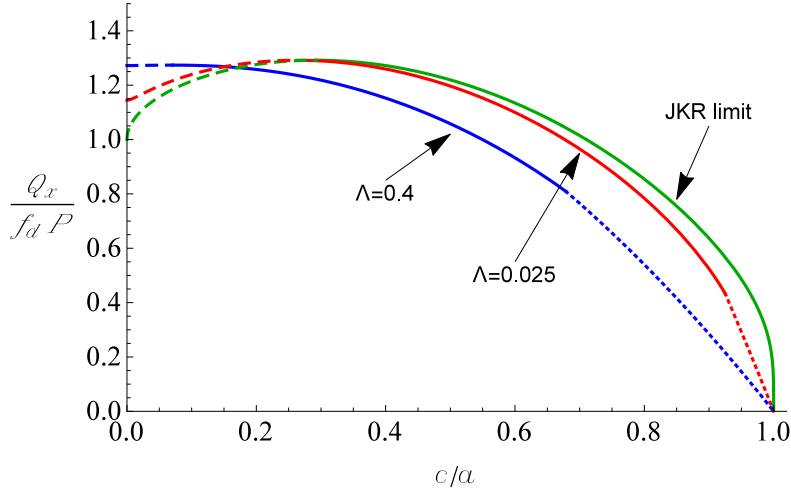
Fig. 5: Comparison of the double Cattaneo-Mindlin solution with the JKR limit for $\psi = 0.1$.

As predicted, the curve for $\Lambda = 0.025$ is very close to the JKR curve, though the maximum Q_x is shifted slightly to the left. Notice incidentally that we might have chosen to plot the double Cattaneo-Mindlin curves as functions of the location of the mid-point $(c + b)/2a$ of the slip-stick transition region, in which case this shift would be much reduced. For larger Λ, the maximum occurs at significantly lower values of c, but Q_{max} is still very well predicted by the JKR theory even for $\Lambda = 0.4$.

Experimental measurements of static friction ceofficient are usually obtained by increasing the applied tangential force until sliding commences. However, it is clear that under these circumstances, microslip is likely to occur before gross sliding commences, and hence in the present geometry such experiments would lead to the static coefficient of friction being identified as Q_{max}/P, which generally differs from f_s.
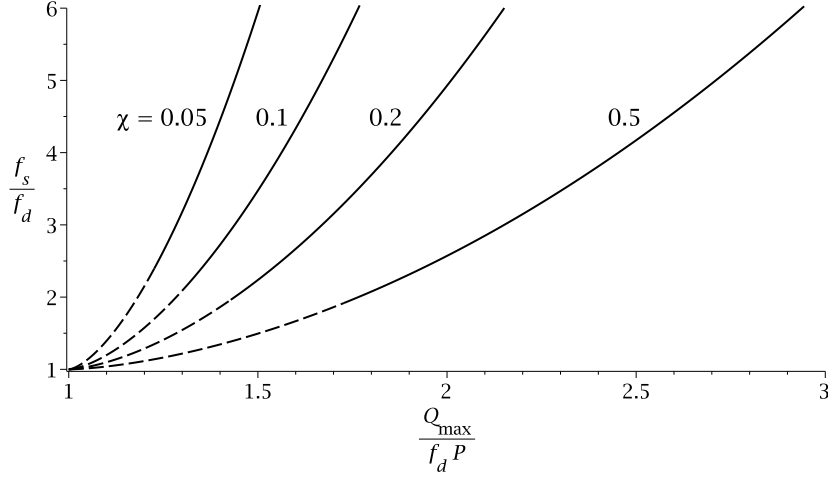
13

Fig. 6: The coefficient ratio f_s/f_d as a function of the apparent ratio $Q_{\max}/f_d\,P$.

Fig. 6 shows the relationship between f_s/f_d and the 'apparent' value of this ratio determined as $Q_{\max}/f_d\,P$, for various values of

$$\chi = \frac{R\Delta}{f_d a^2} = \left(\frac{f_s}{f_d} - 1\right)\Lambda\ . \tag{43}$$

The dashed lines in this figure correspond to ranges in which the small-scale transition criterion $s_0 \ll c$ is not satisfied. We notice that the apparent static friction coefficient is always significantly lower than f_s. The reason of course is that by the time $Q_{\max}$ is reached, a significant part of the contact area has slipped sufficiently to transition to a local coefficient f_d, and the measured coefficient is a weighted average over the whole contact area.

Notice that the limiting case $\chi = 0$ can arise only if $\Delta = 0$, meaning that the transition from f_s to f_d occurs over an infinitesimal slip distance. As explained in §3, the partial slip solution is then identical to the conventional Cattaneo-Mindlin solution with $f = f_d$ and hence slip occurs for $Q = f_d P$ regardless of the static coefficient of friction f_s. This case is defined by the vertical axis in Fig. 6.

7   Conclusions

We have shown that the use of a slip-weakening friction law has a qualitative effect on the solution of microslip problems. The mechanics of the classical Cattaneo-Mindlin problem then have a mathematical structure similar to that of the adhesive contact problem, and we can identify an analogue of the 'JKR' solution, in which the extent of the stick zone is governed by the occurrence of a pressure-dependent mode II stress-intensity factor at the stick-slip boundary. By exploring the two-dimensional Hertzian geometry, we were able to identify the

14

equivalent fracture toughness, which is independent of the detailed goemetry, but proportional to the square root of the local contact pressure. We also defined a length scale s_0 analogous to the small-scale yielding criterion whose value enables us to judge whether the singular solution gives a good approximation to the more exact solution.

The tangential force reaches a maximum before the stick zone has shrunk to zero, at which point there will be a discontinuous change of state to gross sliding. This implies that estimates of the static coefficient of friction from experiments on the inception of sliding will generally significantly underestimate the values appropriate at the microscale.

Acknowledgements

References

[1] Johnson KL. 1961. Energy dissipation at spherical surfaces in contact transmitting oscillating forces, *J. Mech. Eng. Sci.* **3**, 362–368.

[2] Popp K, Panning L, Sextro W. 2003. Vibration damping by friction forces: theory and applications. *J Vib Control,* **9**, 419–448.

[3] Nowell D, Dini D, Hills DA. 2006. Recent developments in the understanding of fretting fatigue. *Eng Fract Mech.* **73**, 207–222.

[4] Rabinowicz E. 1995. *Friction and Wear of Materials*, John Wiley, New York, 2nd. edn.

[5] Popp K., Stelter P. 1990. Stick-slip vibrations and chaos.*Phil. Trans. R. Soc. Lond.,* **332**, 89–105.

[6] Rabinowicz E. 1951, The nature of the static and kinetic coefficients of friction, *J. Appl. Phys.,* **22**, 1373–1379.

[7] Feynman RP, Leighton RB, Sand M. 1964. *The Feynman Lectures on Physics,* Addison-Wesley, Vol. I, 12-5.

[8] Poliakov ANB, Dmowska R, Rice JR. 2002. Dynamic shear rupture interactions with fault bends and off-axis secondary faulting.*J. Geophys. Res.,* **107 (B11)**, Art. 2295.

[9] Rice JR. 1996. Low-stress faulting: Strong but brittle faults with local stress concentrations.*Eos Trans. AGU,* **77** (46), Fall Meet. Suppl., F471.

[10] Bowden FP, Tabor D. 1950. *The Friction and Lubrication of Solids,* Clarendon Press, Oxford, 1950.

[11] Ruina, A. 1983. Slip instability and state variable friction laws. *J. Geophys. Res.,* **88 (B12)**, 10359–10370.

[12] Rice JR, Lapusta N., Ranjith K. 2001. Rate and state dependent friction and the stability of sliding between elastically deformable solids. *J. Mech. Phys. Solids,* **49**, 1865–1898.

[13] Johnson KL. 1985.*Contact Mechanics*, Cambridge University Press, Cambridge.

[14] Cattaneo C. 1938. Sul contatto di due corpi elastici: distribuzione locale degli sforzi. *Rendiconti dell'Accademia Nazionale dei Lincei* **27**, 342–348, 434–436, 474–478. (In Italian)

[15] Mindlin RD. 1949. Compliance of elastic bodies in contact. *ASME J. Appl. Mech.* **16**, 259–268.

[16] Munisamy RL, Hills DA, Nowell D. 1994. Static axisymmetrical Hertzian contacts subject to shearing forces. *ASME J.Appl. Mech.* **61**, 278–283

[17] Ciavarella M. 1998a. The generalized Cattaneo partial slip plane contact problem. I-Theory, II-Examples.*Int.J.Solids Struct.* **35**, 2349–2378.

[18] Jäger J. 1998. A new principle in contact mechanics. *ASME J.Tribology.* **120**, 677–684.

[19] Ciavarella M. 1998b. Tangential loading of general three-dimensional contacts. *ASME J. Appl. Mech.* **65**, 998–1003.

[20] Abercrombie RE. Rice JR. 2005. Can observations of earthquake scaling constrain slip weakening? *Geophys.J. Int.,* **162**, 406–424.

[21] Ben-Zion Y. 2008. Collective behavior of earthquakes and faults: continuum-discrete transitions, progressive evolutionary changes, and different dynamic regimes.*Rev.Geophys.* **46**, RG4006.

[22] Maugis, D. 1992. Adhesion of spheres: The JKR-DMT transition using a Dugdale model. *J. Colloid Interface Sci.,* **150**, 243–269.

[23] Greenwood JA, Johnson KL. 1998, An alternative to the Maugis model of adhesion between elastic spheres. *J. Phys. D: Applied Physics.* **31**, 3279–3290.

[24] Svetlizky I, Fineberg J. 2014. Classical shear cracks drive the onset of dry frictional motion, *Nature* **509**, 205–208.

[25] Ciavarella M. 2015. Transition from stick to slip in Hertzian contact with "Griffith" friction: the Cattaneo-Mindlin problem revisited. *J. Mech. Phys. Solids,* under review.

[26] Rice JR. 1974, Limitations to the small scale yielding approximation for crack tip plasticity,*Journal of the Mechanics and Physics of Solids,* Vol. **22**, 17–26.

[27] ANSYS Mechanical APDL Verification Manual - "VM272: 2-D and 3-D Frictional Hertz Contact", ANSYS, Inc. Release 15.0 November 2013, 785–788

[28] Yang B, Laursen TA., Meng X. 2005, Two dimensional mortar contact methods for large deformation frictional sliding.*Int. J. Numer. Meth. Engng.,* **62** 1183–1225. doi: 10.1002/nme.1222